Scientific Research Publishing

International Journal of Geosciences, 2025, 16(8), 540-553
https://www.scirp.org/journal/ijg
ISSN Online: 2156-8367
ISSN Print: 2156-8359

Quantification of a Granite Quarry by Electrical and Seismic Refraction Methods in the Locality of Nonkouagon (South of Ivory Coast)

Yacouba Ouattara[1], Simon Pierre Djroh[1,2*], Donissongou Dimitri Soro[1]

[1]Applied Geophysics Research Team Laboratory, Mineral and Energy Resources, Faculty of Earth Science and Mineral Resources, Félix Houphouët Boigny University, Abidjan, Côte d'Ivoire
[2]Geophysical Research Office Côte d'Ivoire, Abidjan, Côte d'Ivoire
Email: *djrohsp@gmail.com

How to cite this paper: Ouattara, Y., Djroh, S.P. and Soro, D.D. (2025) Quantification of a Granite Quarry by Electrical and Seismic Refraction Methods in the Locality of Nonkouagon (South of Ivory Coast). *International Journal of Geosciences*, **16**, 540-553.
https://doi.org/10.4236/ijg.2025.168026

Received: February 19, 2025
Accepted: August 18, 2025
Published: August 21, 2025

Abstract

This study enabled us to assess the granite potential on the *Nonkouagon* site, with a view to meeting the need for supplies of aggregates (essential materials for infrastructure construction). To do this, we began by identifying the resistant zones, comparable to granitic formations, by means of resistivity maps and 2D profiles using the dipole-dipole device. Next, electrical boreholes were drilled with the Schlumberger device in the vicinity of these zones in order to determine the depositional stratigraphy and therefore the rooting depth of the massive rock, which varies between 6 and 30 m. Indeed, the electrical prospecting made it possible to highlight three lithological groups which are the filling sediments, the volcano-sediments and the basement (granites). The sedimentary formations correspond to the conductive zones, while the basement is represented by resistant zones. Finally, to confirm the results of the electrical method, seismic refraction was performed and the interpretation of the seismic section also showed three geological layers. The roof of the granite is observed from a depth of 16 m with a seismic velocity varying from 4.48 km/s to 4.72 km/s. The overlying layers are characterized by seismic velocity which vary from 3.84 km/s to 4.32 km/s for the saprolite and from 3.61 km/s to 3.76 km/s for the alterite. In addition, modelling of the granite areas made it possible to determine the volume of rock and to estimate the exploitable granite reserve at over one million tonnes.

Keywords

Granite, Quantification, Tomography, Seismic

1. Introduction

The Proterozoic domain of *Côte d'Ivoire* is made up of Birimian rocks [1], mainly volcanics (tholeitic and calc-alkaline), granitoids, volcano-sediments and sediments. These formations are of Palaeoproterozoic age [2] and were emplaced during the Eburnian tectonic-metamorphic event, a major episode of crustal accretion at 2.1 Ga [3]-[6].

Because of their mineralogical composition, granitoids are very resistant materials that are widely used in major construction projects (roads, buildings, etc.). Over the last few decades, the Ivorian government, in its ambition to contribute to the development of infrastructures to satisfy its population both on its road network and in housing, has increased the number of construction works. As a result, the exploitation of granite rock quarries is booming as a result of a permanent and growing demand for products such as aggregates (derived from granite massifs) and cement. It is in this context that this work is being carried out to estimate the granitic potential in the *Nonkouagon* locality using electrical resistivity and seismic refraction measurements.

2. Geographical and Geological Context

Nonkouagon is located in the south of *Côte d'Ivoire*. A village in the *Songon* subprefecture in the commune of *Yopougon*, it is located in the *Agnéby* valley 54 km (north-west) from *Abidjan* (Figure 1).

The climate is sub-equatorial, with a relief marked by the presence of three major geomorphological complexes: the high plateaux, the coastal outcrops and the plains [7].

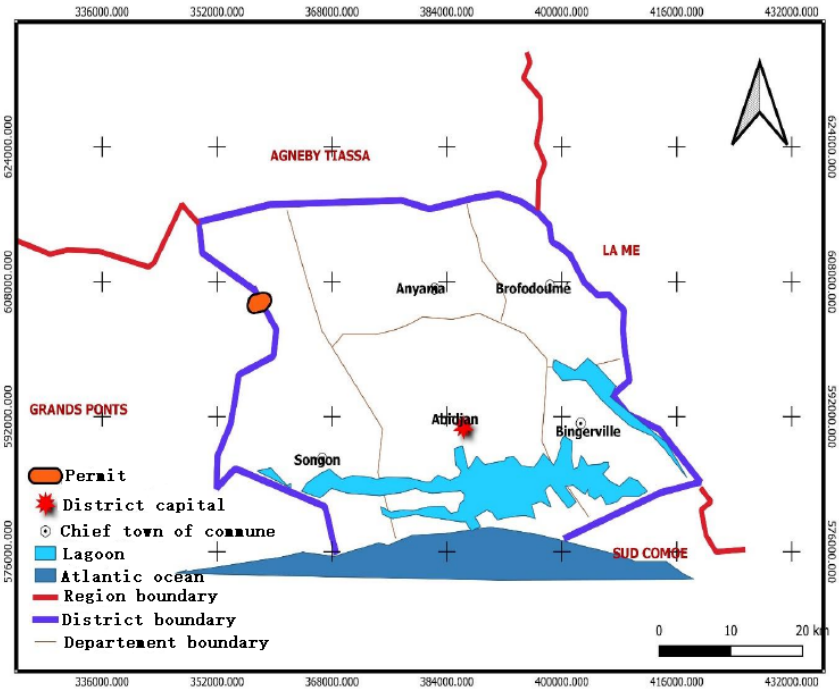

Figure 1. Geographical location of the study area.

Nonkouagon is a contact zone between the formations of the crystalline basement and those of the sedimentary basin [1] [8]-[10]. The geological context of this zone is Birimian (**Figure 2**) and includes fill sediments, volcano-sediments and sub-alkaline granitoids with two micas [11].

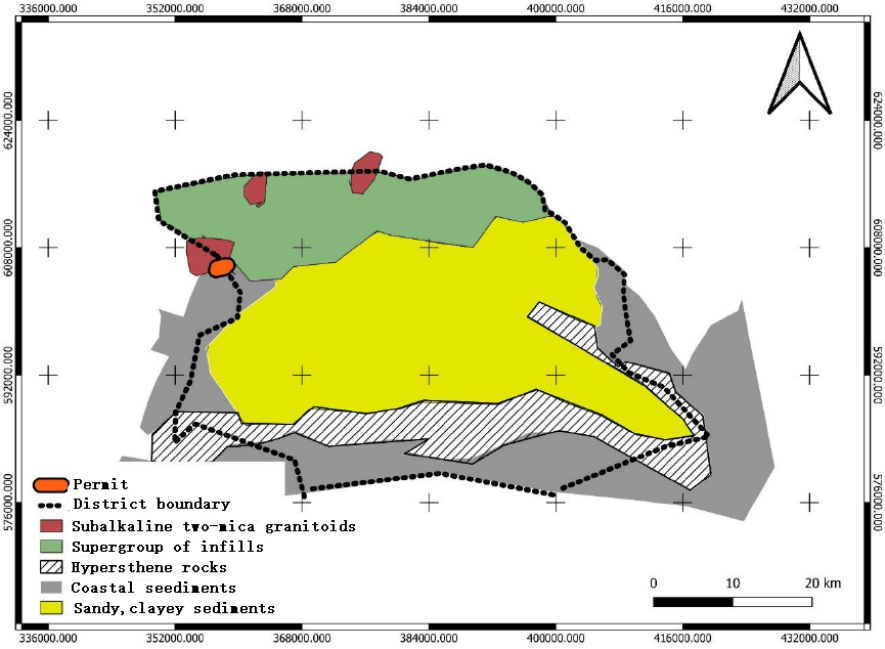

Figure 2. Geological map of the study area [8].

3. Methodology

The principle of electrical prospecting involves injecting an electric current of intensity I into the subsoil using two electrodes (current electrodes). The potential difference ΔV of this current is then measured using two other electrodes (potential electrodes). The apparent resistivity is then obtained from the following expression:

$$\rho_a = k\frac{\Delta V}{I}$$

ρ_a : the resistivity (**Ω.m**);
k : the geometric factor depending on the measuring device (**m**);
ΔV : the measured potential difference (**V**);
I : the intensity of the electric current (**A**).

Electrical tracing is used to determine lateral variations in electrical resistivity; the device used is the dipole-dipole, characterised by an identical spacing between the current injection electrodes (A, B) and the potential electrodes (MN), hence (AB = MN = a). For this study, the SYSCAL PRO resistivity meter was used to emit the current and take the electrical resistivity values, with a spacing of 20 m between the electrodes.

RES2DINV software was used to produce psections showing the true values of apparent resistivity at actual depths. Geosoft can then be used to produce resistiv-

ity maps to assess the horizontal extension of geological formations.

Electrical drilling is a technique used to investigate the subsoil vertically at a given point. It involves taking a series of measurements of the apparent resistivity ρa at the point of interest, keeping the potential electrodes MN fixed and successively moving the current electrodes AB apart. During the implementation of the electrical survey with the Schlumberger device (where MN<<AB), the potential electrodes MN were fixed at 1 metre (*i.e.* MN/2 = 0.5 m) and the separation of the current electrodes AB began from 2 metres (*i.e.* AB/2 = 1 metre) up to AB = 100 m, *i.e.* AB/2 = 50 m. Two clutches were made during this measurement:

- the first at AB/2 = 3 metres, MN/2 is reduced to 1 m;
- the second at AB/2 = 20 metres, MN/2 is reduced to 2 metres.

Inverting the borehole data using IX1D software produces borehole curves, the shape of which can already give an idea of the characteristics of each horizon.

To estimate rock tonnage, we first need to define the granite areas, then determine the volume of rock and finally estimate rock tonnage. The granite areas are delineated using resistivity maps based on depth. The volume of rock is determined from the results of the surface of the granite areas and the average thickness of the granite in each area. This involves multiplying the surface area by the average thickness of the granite [12]. Finally, the tonnage (QG) is determined by multiplying the total volume of rock by the density of the granite, which is 2.67.

The seismic acquisition (seismic refraction) was carried out on a layon (L150) where resistant zones had previously been determined using the electrical method. This acquisition was carried out in order to provide more precise information about the competent rock. Five shots were fired at specific locations (**Figure 3**), in order to study the variation in seismic wave propagation times as a function of the distance separating the signal recording point and the shooting point where the explosions were made. Variations in seismic velocity are a function of hardness/density, degree of consolidation, water saturation, etc. So we can distinguish between compact rock and solid rock. A distinction can thus be made between compact rock and loose ground, compact rock and weathered rock, fractured zones in sound rock, and the level of the water table [13]-[15].

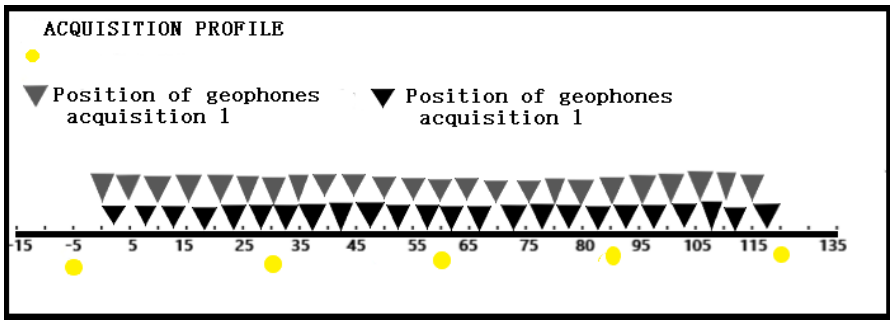

Figure 3. Schematic presentation of the seismic acquisition (the yellow circles represent the shooting points).

A set of 24 geophones connected to the GEODE 24 seismograph were used to record seismic data from hammer blows on a steel plate. Once the number of layers had been determined from the slope breaks on the dromochronics (a curve representing time as a function of propagation distance), the data was inverted to obtain a 2D diagram of seismic wave velocities using SEISMAGER software.

4. Results

The electrical train data provided four resistivity maps with depths of 2, 8, 14, and 20 metres.

The maps at depths of 2 and 8 m (**Figure 4(a)** and **Figure 4(b)**) have the same characteristics and show apparent resistivities that vary from 60 to 2000 Ω.m. Three types of anomalies are highlighted. High resistivity anomalies (from dark red to violet), which can be identified from 1027 Ω.m upwards. Medium resistivity anomalies (yellow to orange) have values between 522 and 984 Ω.m. Low resistivities (blue to green) are below 522 Ω.m.

Structurally, these two maps are not so different as similar fractures (F1, F2 and F4) are found oriented N 70˚, N 108˚, N 15˚ respectively.

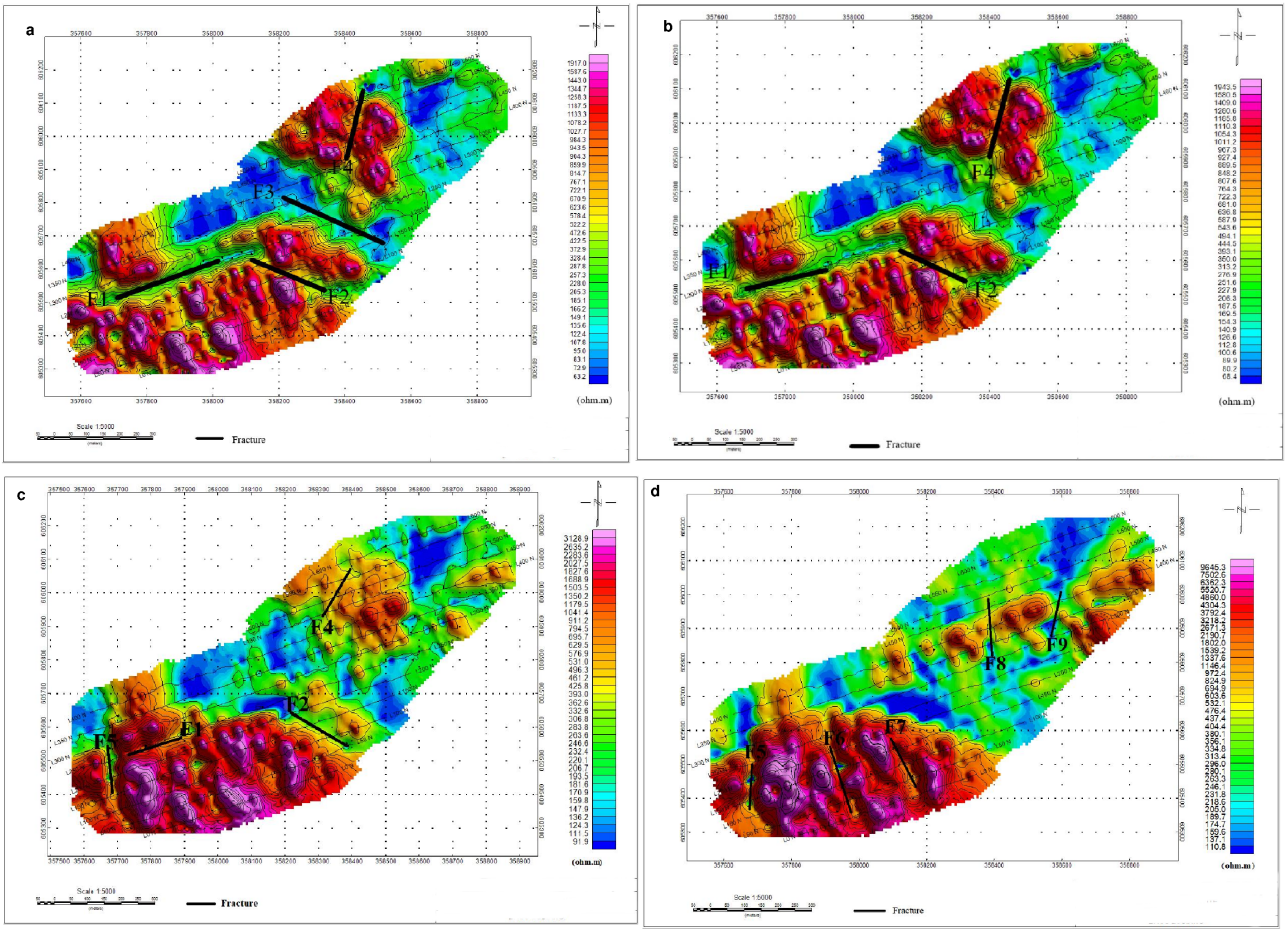

Figure 4. Resistivity map for different depth levels, (a) depth 2 m, (b) depth 8 m, (c) depth 14 m and (d) depth 20 m.

At a depth of 14 m (Figure 4(c)), resistivities vary from 90 to 3128 Ω.m. Zones of high resistivity are above 1350 Ω.m while zones of medium and low resistivity are between 425 and 1179 Ω.m; 90 Ω.m and 425 Ω.m respectively. Four fractures are highlighted, F1, F2, F4 and F5 oriented N 70˚, N 112˚, N 50˚ and N 15˚ respectively.

Resistivities at 20m depth (Figure 4(d)) vary between 110 and 9645 Ω.m. The resistive zone has a value greater than 2000 Ω.m. The average resistivity zone is between 476 Ω.m and 1800 Ω.m. Finally, the conductive part has values between 110 Ω.m and 476 Ω.m. At this depth, the granite is still affected by several fractures ranging in orientation from N 15˚ to N 150˚.

The resistant anomaly in the upper part (to the north) of the 2 and 8 m deep maps appears to be very superficial because it disappears with depth.

With regard to the inverse sections of the electrical resistivity tomography, 04 profiles (L0, L200, L400, L600) out of 13 profiles were selected to present the geoelectrical structure of the subsoil (Figure 5). All these profiles are oriented SW-NE.

Along profile L0 (Figure 5(a)), the roof of the high-resistivity zone is rooted from 20 m upwards, with the exception of station −360 where a resistant part is found at the surface (7.5 m) due to a discontinuity between the moderately resistant zones. The non-rooted zones have a lower electrical resistivity because they are exposed to strong weathering. These would be lateritic layers.

On the reverse section of profile L200 (Figure 5(b)), the bedrock extends from stations −590 to −80. The top of the bedrock is rooted at 20 m but in some places, it is found at 10m. A fracture occurs at 20m at station −540.

Profile L400 (Figure 5(c)) shows pockets of bedrock rooted in conductive layers. The areas of low resistance observed on the surface represent weathered bedrock.

The resistivity section L600 (Figure 5(d)) also shows resistant zones on the surface. Given the position of this bedrock, it would hypothetically have undergone alteration.

Electrical survey

The electrical tracings highlighted anomalies indicating the presence of lithological contacts and fractures. The electrical boreholes (Figure 6) give an idea of the number of terrains (geological layers) and their respective thicknesses, with a view to estimating the depth of the sound basement roof (granite roof). In the course of this study, four (04) of the 15 electrical boreholes (EB) were drilled.

The boat-shaped sounding curves (type H), represented by SE6 (Figure 6(a)), show 3 horizons, the first of which is the weathering layer, the underlying horizon is slightly weathered and not very conductive (saprolite). The last horizon is resistant and represents the sound bedrock at a depth of 8 m. The first and second layers are 1 m and 7 m thick respectively. The sound bedrock begins at a depth of 8 m.

Hole SE4 (Figure 6(b)) shows a KH-type curve with a weakly resistant overburden 2.5 m thick. A layer (saprolite) lies underneath with low resistance. The sound bedrock follows at 3.5 m but is altered from a depth of 6 m.

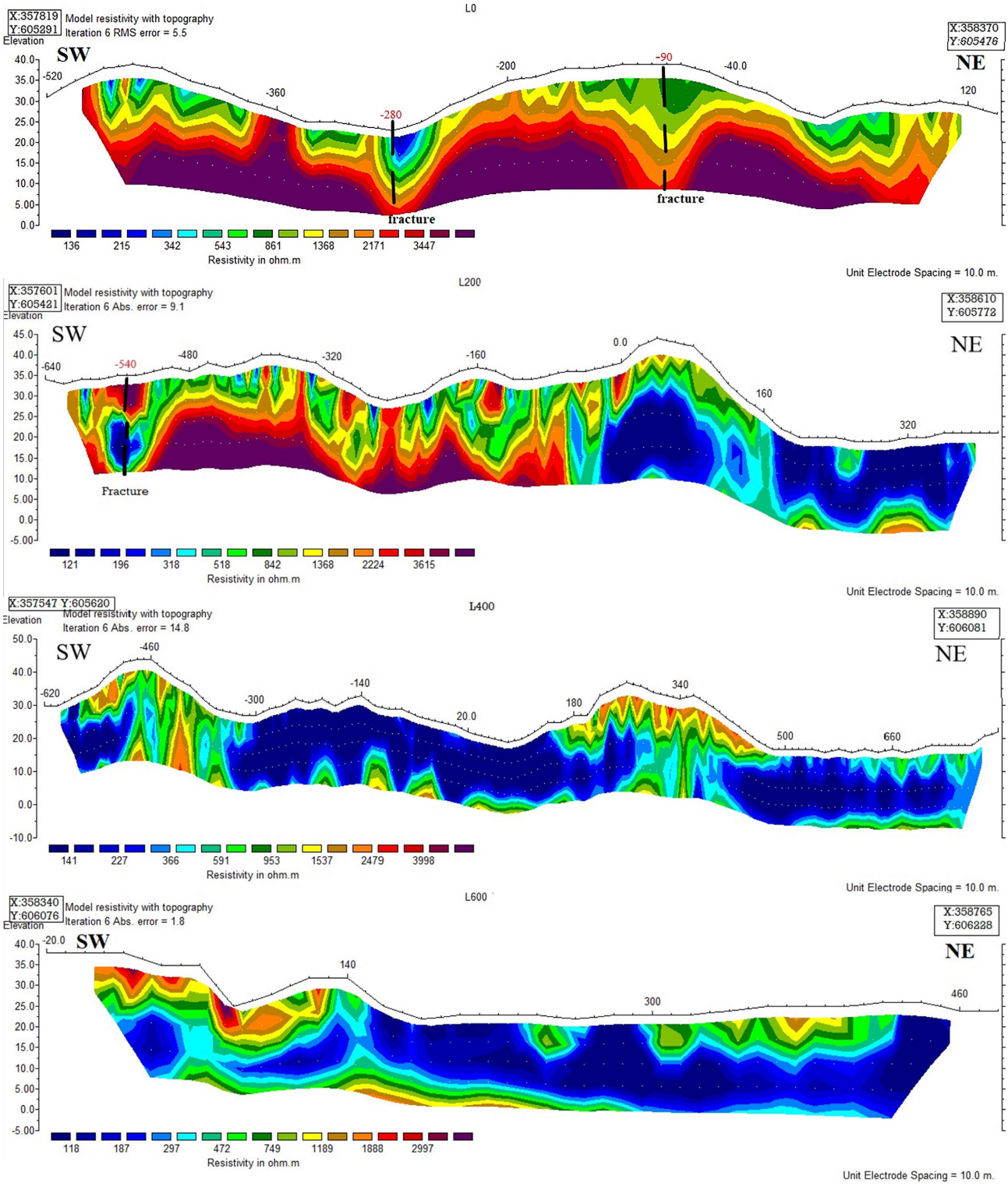

Figure 5. Inverse sections of profiles L0 (a), L200 (b), L400 (c) and L600 (d).

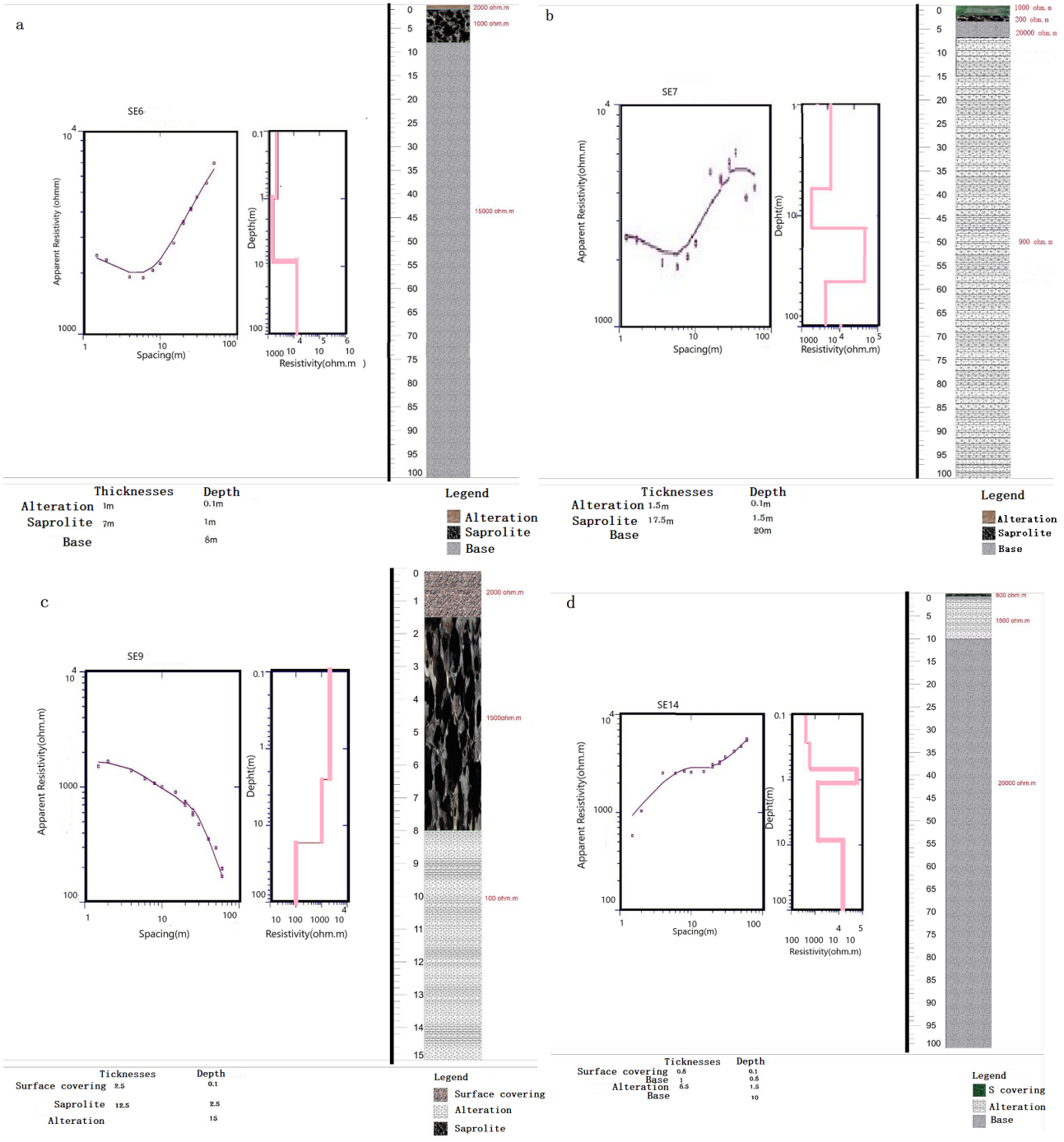

Figure 6. Different types of sounding curve: Type H (a); KH (b); Q (c); A (d).

We also observe another type of drilling curve (SE11) characterised by a decrease in resistivity with depth (**Figure 6(c)**). This is represented by a Q-type curve. The resistant formations are superficial without, however, exceeding the 2000 Ω.m mark. Rooted formations are in the order of 100 Ω.m.

Type A curves are also observed at the SE14 boreholes (**Figure 6(d)**). Three horizons stand out, a superficial overburden, followed by rock weathering and finally healthy granite, the roof of which is at a depth of 10 m.

Table 1 summarises the thicknesses of the different layers at the various drilling points. For boreholes SE9, SE10 and SE11, there is an absence of sound bedrock due to the decrease in resistivity with depth.

Table 1. Summary thicknesses of the various layers at the electrical survey's points.

Electrical Survey	S1	S3	S4	S5	S6	S7	S9	S10	S11	S13	S14	S15
Depth of weathering (m)	6	18	9.5	6	8	20	-	-	-	30	10	10
Granite thickness (m)	94	82	2.5	94	92	80	-	-	-	70	90	90

Based on the drilling data, maps of granitic areas have been drawn up for each depth level (Figure 7). They show the potentially exploitable zones from which the volume can be deduced.

The maps at shallow depths (2 and 8 m) show a good (homogeneous) concentration of resistant formations, corresponding to granite in the northern part (Figure 7(a) and Figure 7(b)), while there is a high concentration of these granite

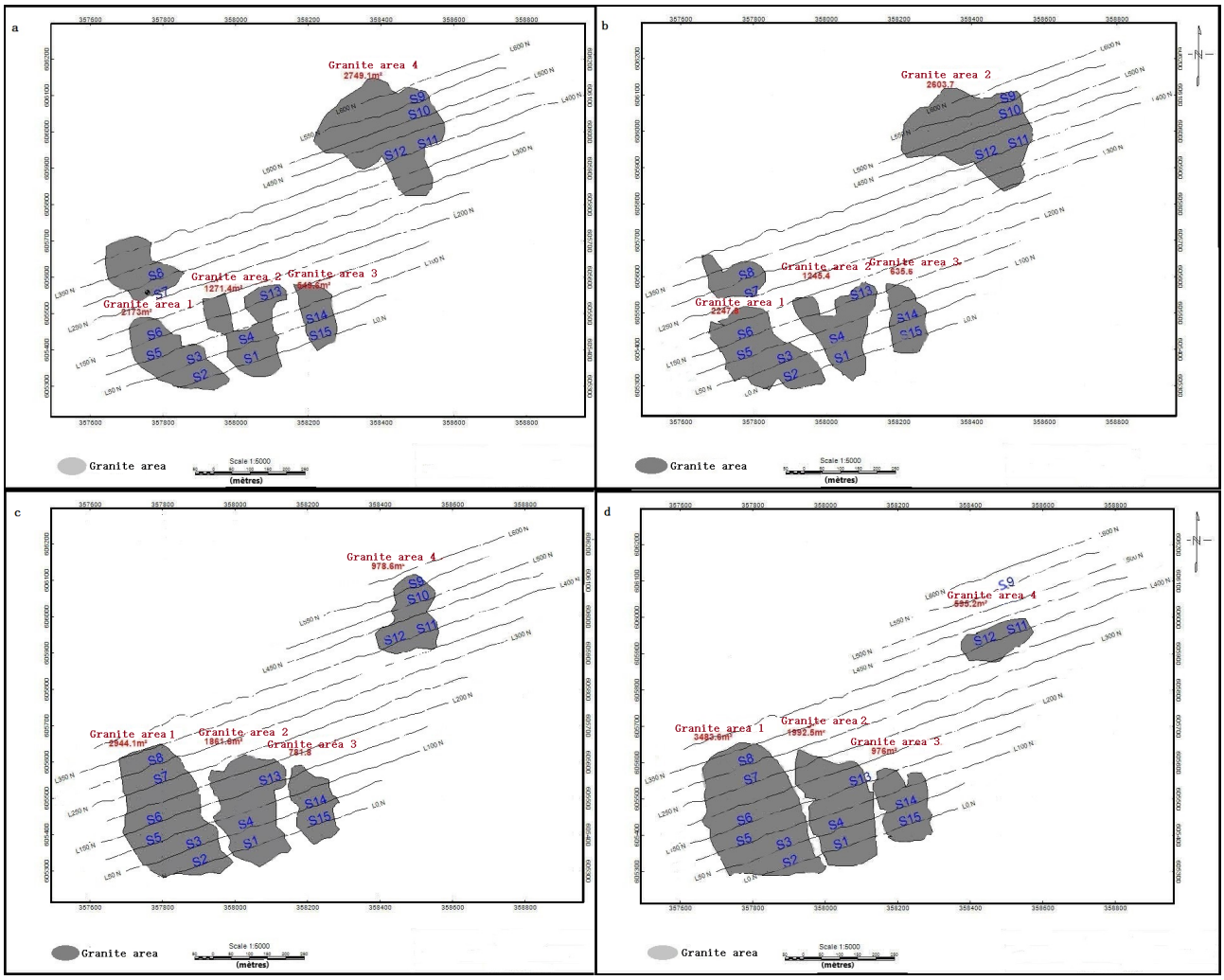

Figure 7. Map of 4 level granitic areas: a (2 m), b (8 m), c (14 m) and d (20 m).

blocks to the west of the prospect compared with the other sectors at increasingly greater depths (Figure 7(c) and Figure 7(d)).

Given the heterogeneity of the subsoil, it is advisable to average the granitic areas at the different depth levels (2 m, 8 m, 14 m and 20 m), which allows us to estimate the buried reserves used to calculate the volume (Table 2).

Table 2. Estimate of buried reserves (the results of some boreholes, such as 9, 10 and 11 are not suitable for quantification because of the absence of sound base).

Area	Electrical surveys	Average granite thickness (m)	Surface area (m^2)	Volume (m^3)
Aire 1	S1, S6, S7	85	2712.1	230528.5
Aire 2	S1, S4, S13	55.5	1592.7	88394.9
Aire 3	S14, S15	90	735.75	66217.5
Aire 4	S9, S10, S11	-	1731.6	-

Adding together the volumes specific to each granite area gives the total rock volume which is 385104.9 m^3.

Once the volume has been determined, we can easily estimate the tonnage.

QG = 385104.9 × 2.67

QG = 1028326.2 t

2.67 being the density of the granite and QG is the tonnage of granite.

Seismic profiling of the granite

The seismic profile, 120 m long, was made between stations −600 and −480 on the layon L150. The profile (Figure 8(a)) shows the presence of three distinct terrains (alterite, saprolite and basement). The top of the basement begins at 16m at the pk −600 station, but the top is more visible at the surface from the pk-510 station.

The seismic section (Figure 8(b)) also shows three distinct tabular zones depending on the speed of the seismic waves. The roof of the granite is easily distinguishable from 16 m upwards, thanks to a deepening red colouration. The seismic speed varies from 4.48 km/s to 4.72 km/s. The overlying layers characterised by green and yellow colours are saprolite and alterite respectively. The seismic velocities revealed vary from 3.84 km/s to 4.32 km/s for the saprolite and from 3.61 km/s to 3.76 km/s for the alterite. The saprolite is 10m thick, while the alterite is 6 m thick.

In view of these results, we can say that the electrical prospecting and seismic refraction methods are complementary and can be used either together (for greater precision) or one in place of the other.

5. Discussion

The combined application of different geophysical prospecting methods (electrical resistivity and seismic refraction) has made it possible to highlight information on the petrophysical characteristics of the *Nonkouagon* subsoil.

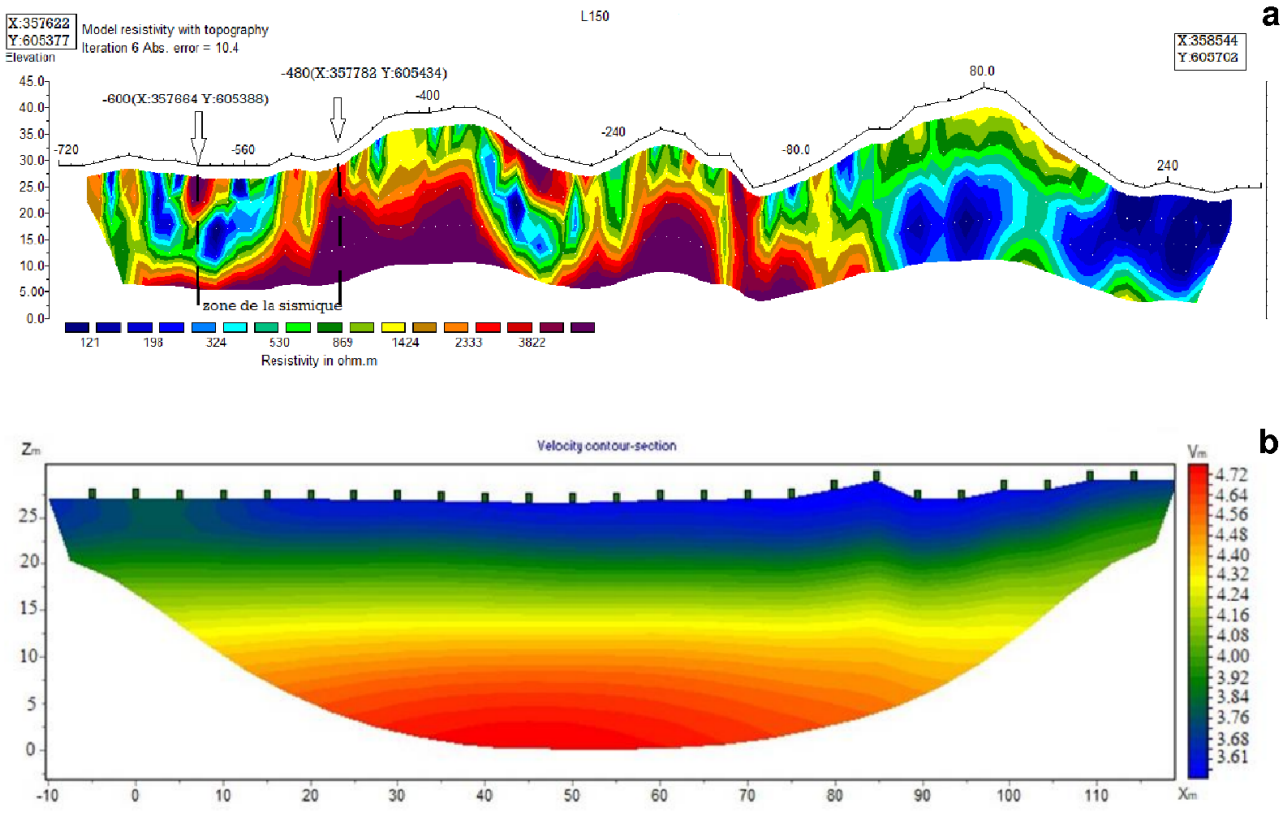

Figure 8. 2D profile of line 150 (a) and seismic section (b).

Electrical prospecting uses variations in electrical resistivity to obtain information about lithological variations in the subsoil [16] [17]. Thus, after electrical profiling, three lithological sets were observed, as in the research results of [18] in the *Sikensi* department. These are fill sediments, volcano-sediments and granites.

The sedimentary formations, conductive zones of varying thickness observed on the resistivity maps, correspond according to [19] to a system of fluvial deposits. In fact, the *Nonkouagon* area has a humid climate that causes strong weathering. The virtual absence of outcrops is due to the presence of an alteration mantle covering the granite. This alteration mantle is highlighted by 2D images and its resistivity does not exceed 1500 Ω.m.

Like [20], our borehole results allowed us to assess a quarrying thickness of more than 50 metres. Thus, based on the work of [12] [21], a rock volume is estimated by performing the product of the surface area of resistant zones by their depth. This calculation technique, which is effective for estimating the volume of a rock mass, was used in our study to quantify the *Nonkouagon* prospect.

The conductive and resistant structures are oriented NE-SW, with a concentration of resistant formations to the south-west. This orientation is the same as the orientation of the structures highlighted during [8] research into the orientation of the Birimian formations (NE-SW).

In addition to this technique for quantifying the granitic massif, there is another equally effective way of calculating rock tonnage: the voxel method [17] [22]. This

is a three-dimensional modelling technique that shows both a 3D model and the volume of the formations being investigated.

The combined use of different geophysical methods gives a fairly accurate idea of the rooting of geological formations. For example, to determine the precise nature of the geological contacts between the basic and ultrabasic rocks in the Bay of Audierne, [23] used seismic refraction in addition to the magnetic method. In our case, in addition to electrical prospecting, seismic refraction was used experimentally to confirm the presence of bedrock.

The top of this granite was observed at a depth of 16 m with a seismic velocity slightly exceeding 4.5 km/s, demonstrating that this granite is of good quality. Studies on the petrophysical characteristics of rocks as a function of seismic velocity by [24] have shown that the higher the resistivity, the higher the seismic velocity Vp. This is the case for our granite section where, during drilling (S6 and S13) on line L150, the resistivity measured was high (>10,000 Ohm) and the seismic velocity in the order of magnitude of (4.72 km/s).

6. Conclusions

The aim of this work was to assess the granitic potential of the *Nonkouagon* locality with a view to meeting aggregate supply needs. Electrical resistivity measurements (drag and borehole) were used to monitor lateral and vertical variations in conductive and resistant zones, while highlighting the presence of layers of alterite, saprolite and sound rock.

The top of the massive rock lies at a depth of between 6 and 30 metres. To confirm the presence of the rock, a seismic refraction study was carried out and the interpretation of the seismic section showed the presence of granite from 16 m.

Modelling of the granite zones enabled us to determine the volume of rock and estimate the exploitable granite reserve at over one million tonnes. However, in some places, there are fractures that could compromise mining if they contain water.

Conflicts of Interest

The authors declare no conflicts of interest regarding the publication of this paper.

References

[1] Bessoles, B. (1977) Geology of Africa: The West African Craton. BGRM.

[2] Plumb, K.A. (1991) New Precambrian Time Scale. *Episodes*, **14**, 139-140. https://doi.org/10.18814/epiiugs/1991/v14i2/005

[3] Abouchami, W., Boher, M., Michard, A. and Albarede, F. (1990) A Major 2.1 Ga Event of Mafic Magmatism in West Africa: An Early Stage of Crustal Accretion. *Journal of Geophysical Research*: *Solid Earth*, **95**, 17605-17629. https://doi.org/10.1029/jb095ib11p17605

[4] Liégeois, J.P., Claessens, W., Camara, D. and Klerkx, J. (1991) Short-Lived Eburnian Orogeny in Southern Mali. Geology, Tectonics, U-Pb and Rb-Sr Geochronology. *Precambrian Research*, **50**, 111-136. https://doi.org/10.1016/0301-9268(91)90050-k

[5] Boher, M., Abouchami, W., Michard, A., Albarede, F. and Arndt, N.T. (1992) Crustal Growth in West Africa at 2.1 Ga. *Journal of Geophysical Research: Solid Earth*, **97**, 345-369. https://doi.org/10.1029/91jb01640

[6] Vidal, M., Delor, C., Pouclet, A., Simeon, Y. and Alric, G. (1996) Geodynamic Evolution of West Africa between 2.2 Ga and 2 Ga: The "Archean" Style of the Green Belts and Birimian Sedimentary Complexes of Northeastern Côte d'Ivoire. *Bulletin de la Société Géologique de France*, **167**, 307-319.

[7] Verniere, M. (1969) Monograph of the Semi-Urban Center of Anyama, Côte d'Ivoire, Volume 1: The Environment and People. Overseas Scientific Research Office.

[8] Tagini, B. (1971) Structural outline of Côte d'Ivoire. Essay on Regional Geotectonics. State Doctoral Thesis in Natural Sciences, University of Lausanne (Switzerland) and SODEMI.

[9] Camil, J. (1984) Petrography, Chronology of Archean Granulitic Assemblages and Associated Formations of the Man Region (Ivory Coast): Implications for the Geological History of the West African Craton. State Doctorate Thesis in Natural Sciences. University of Cocody-Abidjan, Côte d'Ivoire.

[10] Delor, C., Ibrahima, D., Tastet, J.P., Yao, B., Siméon, Y., Vidal, M. and Dommanget, A. (1992) Geological Map of Côte d'Ivoire at 1: 200,000, Abidjan Sheet. Geology Department, Abidjan, Côte d'Ivoire.

[11] Palé, S.H. (2019) Contribution of the Electrical Resistivity Method in the Quantification of a Granite Complex for Industrial Exploitation: Case of Bago, North-West Abidjan Côte d'Ivoire. Master's Thesis, Université Félix Houphouët-Boigny.

[12] Kouakou, A.K., kouamé, N.L., Djroh, S.P., kouadio, L.K. and Sombo, C.B. (2017) Use of the Electrical Resistivity Method for the Search for Granite Quarries and Estimation of Rock Tonnage on Three Sites: Ayamé, Bouaké and Ferkessédougou, Côte d'Ivoire. *International Journal of Technical Research and Applications*, **5**, 40-46.

[13] Bourbié, T., Coussy, O. and Zinszner, B. (1986) Acoustics of Porous Media. Technip.

[14] Guéguen, Y. and Palciauskas, V. (1992) Introduction to Rock Physics. Hermann.

[15] Belghoul, A (2007) Petrophysical and Hydrodynamic Characterization of the Crystalline Basement. Doctoral Thesis in Geophysics, University of Montpellier II-Sciences and Technology of Languedoc.

[16] Aka, E.B.J.C. (2018) Geophysical Study Using Magnetometry and Induced Polarization of Precambrian Formations in the GOUMERE Region (Northeastern Côte d'Ivoire): Lithostructural Characterization and Implications for Understanding Gold Mineralization. PhD Thesis, Université Félix Houphouët-Boigny.

[17] Djroh, S.P., Aka, E.B.J.C., Ouattara, Y., Gnoleba, S.P.D., Ahade, Y.M.A. and Kouame, L.N. (2022) Tomographie électrique et estimation des réser ves de Granite pour une exploitation de carrière à Brofodoume, Sud-Est de la Côte d'Ivoire. *Journal of the Cameroon Academy of Sciences*, **18**, 437-446. https://doi.org/10.4314/jcas.v18i2.4

[18] Sombo, P., Kouassi, F.W., Sombo, B.C., Kouamé, L.N. and Kouakou, K.E.G. (2011) Contribution of Electrical Prospecting to the Identification and Characterization of the Basement Aquifers of the Sikensi Department (South of Côte d'Ivoire). *European Journal of Scientific Research*, **64**, 206-219.

[19] Touré, S. (2007) Petrography and Geochemistry of the Bondoukou Granitoid Massif Northeastern Côte d'Ivoire. Magmatic Evolution and Geodynamic Context in the Lower Proterozoic. Relationship with the volcano-Sdetritic Zanzan, Koun, Tanda attributed to the Tarkwaiian of Ghana. Paleogeographic Implications. Doctoral Thesis, Université d'Abobo-Adjamé.

[20] Kouakou, E.G.K., Sombo, B.C., Digbéhi, Z.B., Kouassi, F.W., Sombo, A.P. and Kou-

amé, L.N. (2012) Use of Geophysical Prospecting by Electrical Resistivity for the Search for Groundwater in the Department of TANDA (Eastern Côte d'Ivoire). *European Journal of Scientific Research*, **83**, 230-244.

[21] Ada, H. (2006) Three-Dimensional Modeling of Rock Masses Using Electrical Imaging Techniques: Application to the Andalamby, Ankilibobo, and Ereheta Quarries on 13th Street, Antananarivo, Madagascar.

[22] Djroh, S.P. (2014) Geophysical Studies of the Samapleu Cupronickeliferea Platinoid Deposit. 3D Modeling Attempt by Interpreting Magnetic and Electrical Data. Doctoral Thesis, Université Félix Houphouët-Boigny.

[23] De Poulpiquet, J. (1988) Magnetic and Seismic Study of the Basic and Ultrabasic Massif of Audierne Bay (Armorican Massif). *Geology of France*, **4**, 11-22.

[24] Kouamé, L.N., Sombo, B.C., Digbehi, Z.B., Sombo, A.P., Kouassi, G. and Essoh, A.S. (2011) Seismic Velocity-Petrophysical Properties Relationships of Sedimentary Terrains in the Continental Margin of Côte d'Ivoire. *Geo-Eco-Trop*, **35**, 9-12.